

Electrical Behavior and Structure of Polypropylene/Ultrahigh Molecular Weight Polyethylene/Carbon Black Immiscible Blends

I. MIRONI-HARPAZ, M. NARKIS

Department of Chemical Engineering, Technion Israel Institute of Technology, Haifa 3200, Israel

Received 23 June 2000; accepted 9 August 2000

ABSTRACT: This study investigates the electrical behavior, which is the positive temperature coefficient/negative temperature coefficient (PTC/NTC), and structure of polypropylene (PP)/ultrahigh molecular weight polyethylene (UHMWPE)/carbon black (CB) and PP/ γ irradiated UHMWPE (XL-UHMWPE)/CB blends. As-received UHMWPE or XL-UHMWPE particles are chosen as the dispersed phase because of their unusual structural and rheological properties (extremely high viscosity), which practically prevent CB particles penetration. Because of their stronger affinity to PE, CB particles initially form conductive networks in the UHMWPE phase, followed by distribution in the PP matrix, thus interconnecting the CB-covered UHMWPE particles. This unusual CB distribution results in a reduced electrical percolation threshold and also a double-PTC effect. The blends are also investigated as filaments for the effect of shear rate and processing temperature on their electrical properties using a capillary rheometer. Because of the different morphologies of the as-received and XL-UHMWPE particles in the filaments, the UHMWPE containing blends exhibit unpredictable resistivities with increasing shear rates, while their XL-UHMWPE containing counterparts depict more stable trends. The different electrical properties of the produced filaments are also related to differences in the rheological behavior of PP/UHMWPE/CB and PP/XL-UHMWPE/CB blends. Although the flow mechanism of the former blend is attributed to polymer viscous flow, the latter is attributed to particle slippage effects. © 2001 John Wiley & Sons, Inc. *J Appl Polym Sci* 81: 104–115, 2001

Key words: conductive plastics; immiscible blends; positive temperature coefficient effect; carbon black; polypropylene; ultrahigh molecular weight polyethylene

INTRODUCTION

One of the most common additives used in conducting plastics is carbon black (CB), which initially forms isolated structures within the matrix; then isolated clusters form, and finally through-going paths arise. A through-going path is a continuous network of conducting particles in suffi-

ciently close proximity to allow electrons to flow throughout a specimen. The critical amount of CB necessary to form a conductive network is referred to as the percolation threshold.¹ It is desirable for the conducting filler content to be as low as possible to achieve good processability, good mechanical properties, and low cost. The approach undertaken to reduce the CB content is by formation of segregated CB structures. Thus, the dispersion of CB particles in a semicrystalline polymer, where the CB is localized in the amorphous regions, results in a percolation threshold

Correspondence to: M. Narkis (narkis@tx.technion.ac.il).

Journal of Applied Polymer Science, Vol. 81, 104–115 (2001)
© 2001 John Wiley & Sons, Inc.

decrease.² A binary immiscible blend can be designed in a way that favors the dispersion of CB particles in the minor component of a cocontinuous blend, or even better, at the interfaces.^{2,3} The conductivity and percolation threshold are affected by polymer properties such as viscosity,⁴ surface tension,^{4,5} polymer crystallinity,² and processing.^{6,7}

An interesting phenomenon exhibited by some conductive polymers is a positive temperature coefficient (PTC) effect. The main feature of PTC materials is that heating causes the conductive system to show a sharp resistivity increase near the melting region of a semicrystalline polymer matrix.^{8–18} The PTC effect is sometimes followed by a negative temperature coefficient (NTC) effect, which is a resistivity decrease.^{9–12} PTC materials can be used as self-regulating heaters, current limiters, over-current protectors, microswitches, sensors, and so forth.¹³

A comprehensive theory describing the PTC/NTC phenomenon is not available, although many researchers have tried to explain it.^{11,13–17} Models are largely based on the motion of CB particles and their redistribution during crystallite melting, volume expansion, and viscosity reduction, which occur upon reaching and entering the crystalline melting zones. The most common explanation for the PTC effect is that as the melting temperature is approached, conductive paths are broken due to volume expansion of the polymer matrix. Above the melting temperature, CB particles cluster because of their tendency to agglomerate. This consequently results in the formation of new paths, thus giving rise to the NTC effect.^{9,10,12} The desired PTC performance, which includes a low room temperature resistivity, high PTC intensity, low NTC intensity, and high reproducibility, together with a low filler content can be approached by employing immiscible polymer blends instead of a single polymer system, thus expanding the possibility of tailoring the PTC performance using conductive blends.

The immiscible blend morphology was found to greatly affect the PTC and NTC behavior.¹⁸ When CB is entirely localized in the matrix, the PTC behavior is essentially the same as in a CB-filled single polymer blend.^{19–21} Another interesting possibility is the localization of CB particles solely at the interface of the immiscible polymer blend. Feng and Chan²² reported that in a polypropylene/ultrahigh molecular weight polyethylene (PP/UHMWPE) system, representing an immiscible blend of two semicrystalline polymers, a dou-

ble-PTC effect was observed. There were two sharp jumps in resistivity at the melting temperatures of the two semicrystalline polymers, which were due to the large thermal expansion of the polymers at those temperatures. After the second PTC effect, a sharp NTC effect takes place, similar to that of a CB-filled single semicrystalline polymer.

In this study, neat (serving as references) and CB-containing PP/UHMWPE blends were studied. UHMWPE powders, as-received or γ -irradiated (XL-UHMWPE), were chosen as unique fillers because of their unusual high viscosity. Thus, using UHMWPE as the dispersed phase in a CB-containing polymer blend generated unique structures with segregated CB particles, which were associated with interesting electrical and thermoelectric properties. The CB content is known to have a significant effect on the PTC intensity of a system, and thus the room temperature resistivity–CB content relationship is used to estimate the composition giving a significant PTC effect. The effect of shear level on the electrical conductivity, morphology, and rheological properties of blends was also investigated.

EXPERIMENTAL

The principal polymers used in this study were PP (C-50E, Carmel Olefins) and an UHMWPE powder (Gur 412, Hoechst). Some of the UHMWPE powder was γ irradiated by a Co⁶⁰ source at a 15-Mrad dose in vacuum at room temperature prior to blending. This was done in order to crosslink the particles, subsequently termed XL-UHMWPE. A highly structured, electrically conductive CB (Ketjenblack EC-300, Akzo) was used as the conductive filler.

All blend ratios described in the text relate to weight ratios.

Blends were prepared by a standard procedure of melt mixing of a dry-blended CB and polymer components in a Brabender Plastograph equipped with a 50 cm³ cell; the components were mixed at 200°C and 50 rpm for approximately 15 min. The resulting blends were subsequently compression molded to obtain 3-mm thick plaques.

Filaments of the blends were obtained using a MCR capillary rheometer mounted on an Instron TT-D machine. A capillary of 5 cm (2 in.) length and 0.127 cm (0.05 in.) diameter was employed. The velocity range of the crosshead, which controlled the filament's exiting velocity from the die,

was 0.05–50 cm/min, which corresponded to an approximate shear rate range of 3–3000/s. Extrudate samples were collected as filaments for electrical resistivity measurements and morphological characterization.

The resistivity measuring method depended on the geometry of the samples that were produced by the different processing methods. Compression molded samples were punched into 5-cm diameter disks, and their volume resistivity was measured (DIN 53596) using a Keithley 614 electrometer and a Keithley 240A voltage supplier. Nickel paint was applied to ensure contact between the sample and the electrodes. Filaments produced by the capillary rheometer were measured by a direct method: silver paint was applied at several locations (about 1 cm apart) on the filaments' surface. The resistance was measured between two silver marks along the specimen, and an average volume resistivity through the sample was calculated. Because of the electrometer's limitation, resistivity measurements larger than $1E8$ ohm-cm were considered unprecise and therefore were neglected.

Thermoelectric measurements were conducted while the samples were placed between two electrodes that are part of a heating device controlled by a Eurotherm 91e controller. The samples were heated at a rate of about $2^{\circ}\text{C}/\text{min}$ and subsequently cooled in air back to room temperature at about the same rate.

The morphology of freeze fractured and microtomed surfaces was characterized by a Jeol JSM 5400 scanning electron microscope (SEM). All samples were gold sputtered prior to observation.

RESULTS AND DISCUSSION

Polymer Blends Morphology

The neat polymer blends were studied at a 70/30 blend ratio, the matrix being PP and UHMWPE or XL-UHMWPE serving as the dispersed phase. The UHMWPE particles were smooth ellipsoids having a characteristic size of a few 10s of microns [Fig. 1(a)]. The particles' surface, as depicted in Figure 1(b), appeared as collapsed fibrils with inlaid nodules having a size of less than $1\ \mu\text{m}$ in diameter. These nodules were remnants of a once developed structure consisting of nodules less than $1\ \mu\text{m}$ in diameter interconnected by very fine fibrils.^{7,23} Although some interaction

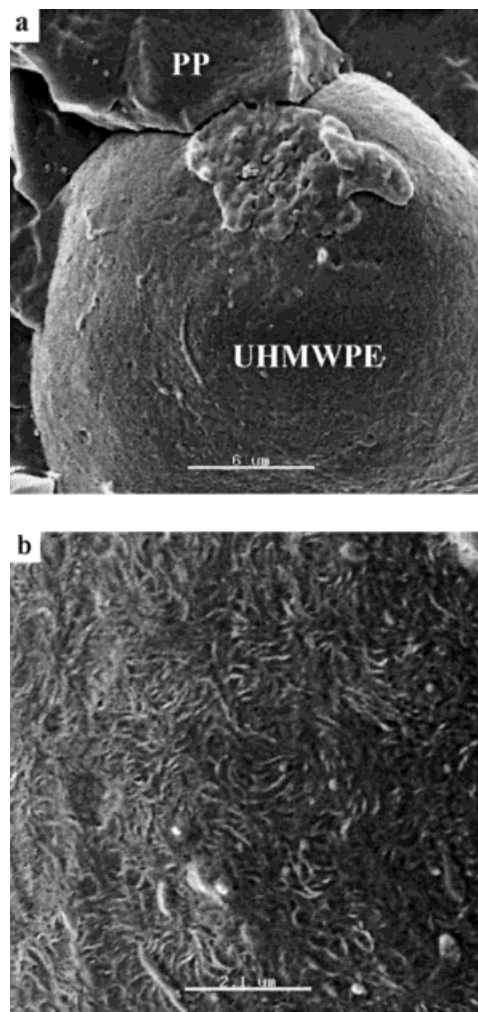


Figure 1 SEM micrographs of freeze fractured 70PP/30UHMWPE blends at two magnifications.

was noticed between the PP and UHMWPE phases, resulting in what seemed to be a part of the matrix adhered to the UHMWPE particle, the adhesion between the two polymers was generally relatively weak, as reflected by the gap at their interface and by the freeze fracture that propagated mostly along the interface of the two polymers.

The blend containing XL-UHMWPE, as depicted in Figure 2, exhibited a different structure than its unirradiated counterpart. Evidently, there was a very good interaction between the PP and XL-UHMWPE particles, as reflected by the lack of a gap at their interface [Fig. 2(a,b)] and by the freeze fracture that propagated mostly through the XL-UHMWPE particles (not shown). Although the contour of the particles was difficult to observe, the particle size was the characteristic

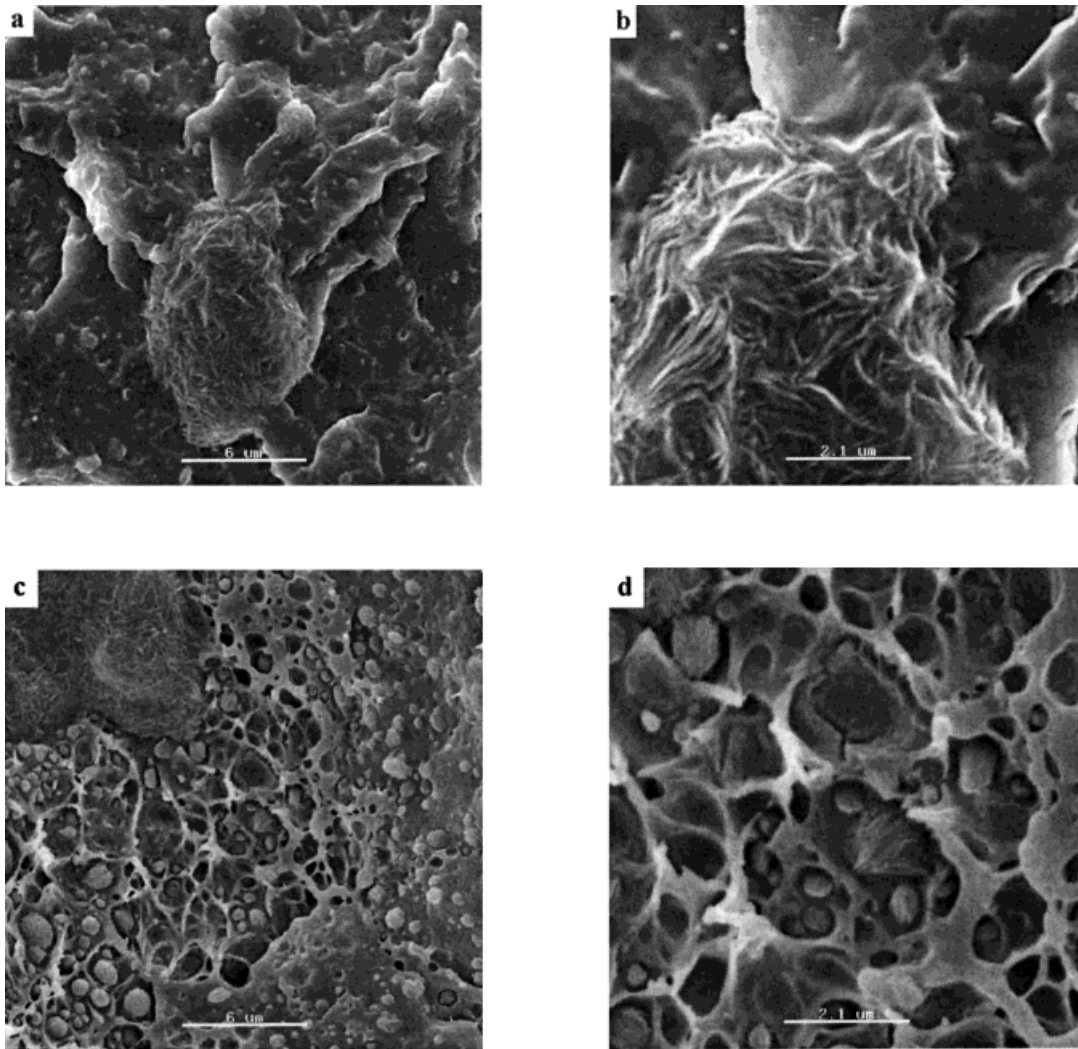


Figure 2 SEM micrographs of 70PP/30XL-UHMWPE blend: (a,b) freeze fractured blend at two magnifications and (c,d) microtomed blend at two magnifications.

few 10s of microns in diameter. Careful observation of the XL-UHMWPE particle surface structure revealed it as complex. A surface consisting of a smooth substance, inlaid with small nodules having a sizes of less than 1–6 μm in diameter, was visible. It seemed that the XL-UHMWPE particle was covered with a smooth substance, which was suggested to be the PP matrix. The SEM micrographs of the microtomed sample depicted in Figure 2(c,d) supported this approach. The porous inner structure of the UHMWPE particles was fixated because of γ irradiation, thus consisting of numerous nodules with diameters ranging from less than 1 to 3 μm . Most of the nodules were connected by fibrils; however, some were covered with a substance that seemed to be part of the PP matrix. Thus, the surface layer of

the fixated porous XL-UHMWPE particles was partially penetrated by the PP matrix, resulting in an interlocking structure. The two phases adhered well to each other, making it difficult to distinguish between them and leading to significant mechanical properties.⁷

The morphological features of the 70PP/30UHMWPE/CB and 70PP/30XL-UHMWPE/CB systems are presented in Figures 3 and 4, respectively. As depicted by the SEM micrographs of 2 (not shown) and 4 phr CB filled PP/UHMWPE blends (Fig. 3), CB appeared in the PP matrix and at the external part of the ellipsoidal UHMWPE particles dispersed in the matrix. The adhesion between the two polymers seemed better than the one depicted by the neat blend, and it became stronger with increasing CB content. Thus, the

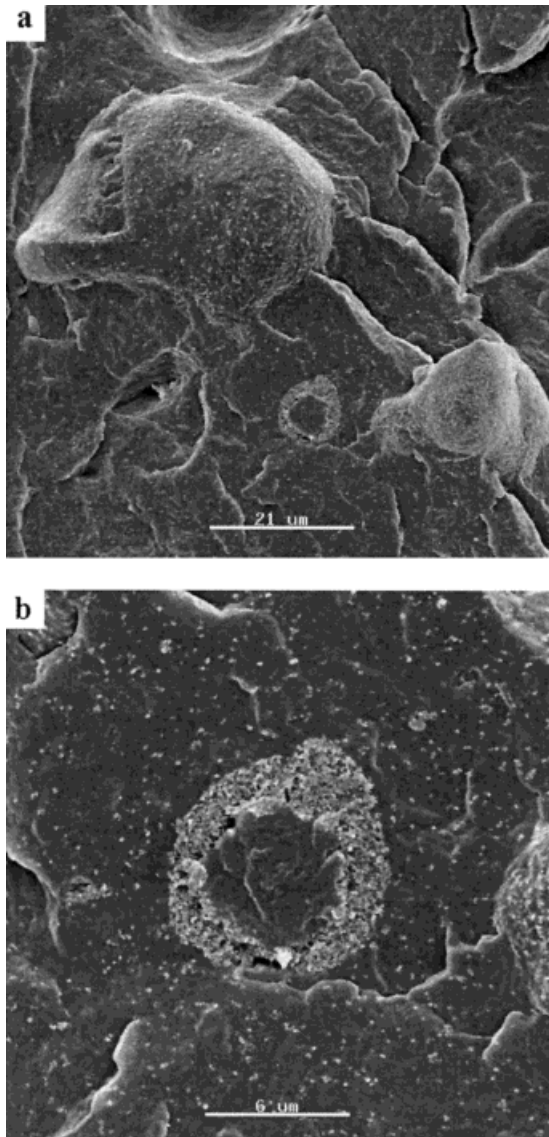


Figure 3 SEM micrographs of freeze fractured 70PP/30UHMWPE/4 phr CB blend at two magnifications.

blend containing 4 phr CB exhibited a very small or no gap between the PE particles and the PP matrix. Introducing CB into the system altered the UHMWPE particle surfaces, which became completely covered by CB, thus changing the surface characteristic of the CB-coated UHMWPE phase, which may have been a reason for the diminished gap. The increased affinity between the matrix and the dispersed phase was also observed by the freeze fracture that propagated through some of the UHMWPE particles, as well as along the interface between the two polymers. Figure 3(b) shows a morphology quite similar to the one described earlier for poly(vinylidene fluo-

ride) (PVDF)/UHMWPE/CB systems.²⁴ The small fractured UHMWPE particle ($\sim 6 \mu\text{m}$ in diameter), seemed to be coated by a rich CB-containing phase, resulting in a core-shell morphology. A similar morphology was previously shown by Feng and Chan,²² who found that CB particles were not only localized in the PP matrix but also accumulated at the interface between the PP matrix and UHMWPE particles. Although CB distributed in both PE and PP phases, it seemed to have a stronger affinity for the PE phase. The tendency of CB particles to preferentially localize in one phase over the other was previously explained by Tchoudakov et al.⁵ to be the result of the stronger affinity of CB to the phase having a higher surface tension. Thus, CB particles have a stronger affinity to the PE phase²⁵ ($\gamma_{\text{PE}} = \sim 36$

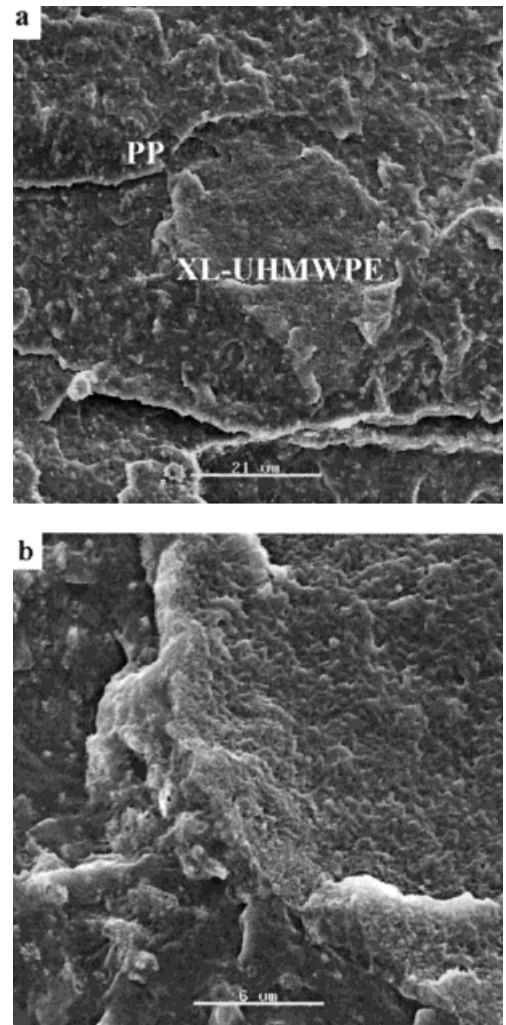


Figure 4 SEM micrographs of freeze fractured 70PP/30XL-UHMWPE/4 phr CB blend at two magnifications.

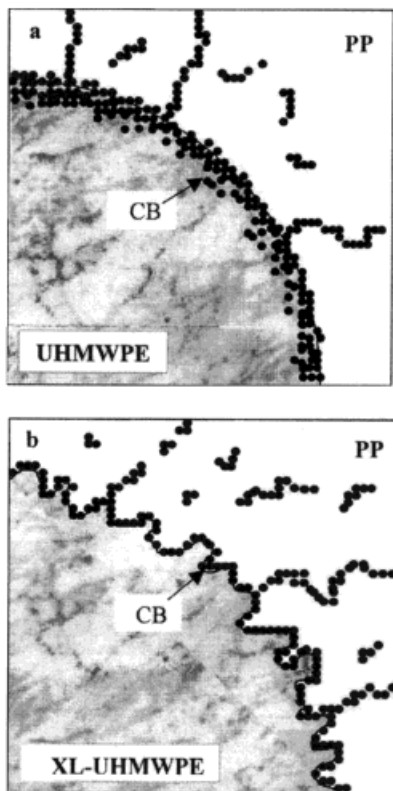


Figure 5 A schematic model of interfaces in (a) PP/UHMWPE/CB and (b) PP/XL-UHMWPE/CB blends.

dyne/cm) than to the PP phase ($\gamma_{PP} = \sim 30$ dyne/cm) as was also found by Sumita et al.³ However, CB particles cannot fully penetrate the highly viscous UHMWPE particles; hence, CB is induced to segregate at the outer skin,^{7,24} establishing a core-shell morphology. The shell is thought to comprise a mixture of PP, less packed regions of the UHMWPE particle, and CB while the core, which is the inner part of the UHMWPE particle, is completely free of CB. When all interfaces between UHMWPE particles and PP are occupied by CB particles, they are forced to be dispersed in the PP matrix.²²

The PP/XL-UHMWPE/CB blends were different from the PP/UHMWPE/CB systems. As previously mentioned, the γ irradiation of the UHMWPE particles fixates their morphology, resulting in porous ellipsoidal elongated shapes, enabling penetration of the PP matrix into the dispersed particles. As depicted in Figure 4(b), CB was located in the PP matrix and at the surface of the XL-UHMWPE particle. CB clusters or CB-covered nodules seemed to be projecting out of the PP matrix, the latter (excluding the CB) depicted also by the neat system (Fig. 2). The developed structure (after melt blend-

ing) of the XL-UHMWPE particle, as opposed to the UHMWPE, provided a different type of interface that was larger in surface area and consisted of many interlocked PP/XL-UHMWPE regions in which CB was presented as well. The inner part of the XL-UHMWPE particle [Fig. 4(b)] was completely free of CB particles. The strong interaction between the two polymers was similar to the one depicted by the neat blend, making it very hard to distinguish between the phases. This strong adhesion was further manifested by the freeze fracture propagating through the PE particles, as seen in Figure 4. The profound difference in CB distribution between the PP/UHMWPE/CB and PP/XL-UHMWPE/CB blends and the interface between UHMWPE particles and PP matrix are depicted by a model in Figure 5, which schematically summarizes the foregoing discussion of the UHMWPE and XL-UHMWPE systems.

Electrical and Thermoelectrical Properties

The volume resistivity of 70PP/30UHMWPE/CB and 70PP/30XL-UHMWPE/CB blends is depicted in Figure 6 as a function of the CB content. The CB-filled PP compound was previously found to percolate at a threshold of about 3 phr CB content, the data referring to the same CB type.⁵ The PP/UHMWPE/CB blend percolated at a 4 phr CB content, whereas the PP/XL-UHMWPE/CB blend had a percolation threshold of about 2 phr CB, a concentration at which the corresponding UHMWPE containing blend was still highly re-

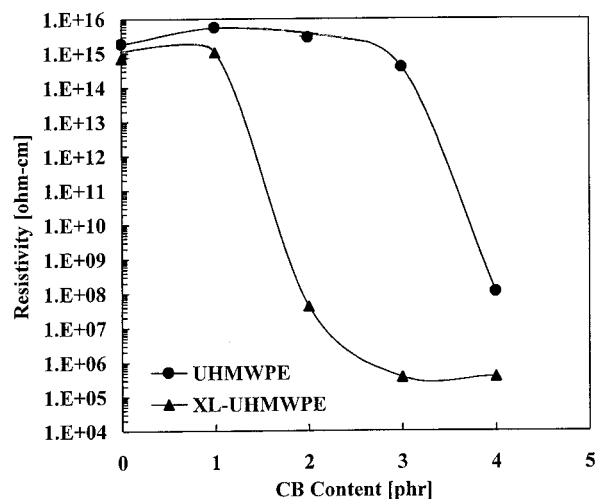


Figure 6 The resistivity versus the CB content of 70PP/30UHMWPE/CB and 70PP/30XL-UHMWPE/CB blends.

sistive. It is known that the electrical properties of immiscible polymer blends are highly dependent on the detailed dispersed particle structure and distribution. Therefore, the difference in percolation thresholds between the as-received and the irradiated UHMWPE particles in the corresponding blends may be discussed in light of the morphology presented in Figures 1–5. Although segregated CB formed chainlike structures on the UHMWPE particles, resulting in conductive networks, UHMWPE particles seemed to be located apart from each other; thus, PE phase continuity (at the 70/30 ratio) within the blend was not established, in agreement with the findings of Feng and Chan.²² They found that phase percolation of UHMWPE within a PP matrix was established at about a 50/50 blend ratio (by weight).²² Therefore, the reduced resistivity obtained at a 4 phr CB content was thought to arise from the establishing of conductive paths through the PP phase, which interconnected the highly CB-covered UHMWPE particles that served as large conductive fillers. Thus, the CB content required to reach the percolation threshold should be enough to cover the UHMWPE particles and to establish conductive paths through the PP matrix.

The PP/XL-UHMWPE/CB blend exhibited a sharp drop in resistivity already at 2 phr CB content. The crosslinked particle having an “infinite” viscosity further induces CB segregation on it, inhibiting the CB particles from penetrating it. Thus, a smaller concentration of CB was needed in order to percolate. Although the preserved developed structure of the XL-UHMWPE particles (Fig. 5) exposed a large surface area, it also enabled some penetration of the PP matrix, resulting in a somewhat higher PE effective content. Thus, the XL-UHMWPE particles were closer to establishing phase continuity, resulting in a required CB content that was lower than the one required to establish conductivity through the UHMWPE blend.

The thermoelectric behavior of 70PP/30UHMWPE/4 phr CB and 2 and 4 phr CB filled 70PP/30XL-UHMWPE blends was investigated. As depicted by Figure 7, upon heating, all investigated samples went through two jumps in resistivity. The 70PP/30UHMWPE/4 phr CB blend showed a sharp jump in resistivity as the sample was heated through the PE melting region, followed by an even sharper jump in resistivity as the sample went through the PP melting region. The NTC effect was not observed due to the samples' prior collapse. The CB-containing 70PP/

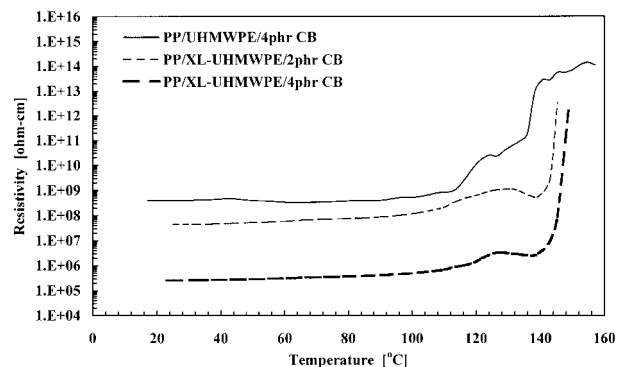


Figure 7 The resistivity versus the temperature curves of 70PP/30UHMWPE/CB and 70PP/30XL-UHMWPE/CB blends.

30XL-UHMWPE blends showed a somewhat different trend upon heating. Only a moderate jump in resistivity as the samples were heated through the PE melting region was observed, followed by a sharp jump in resistivity as the sample reached the PP melting region. However, the second resistivity jump's maximum was not attained and therefore the NTC effect could not be observed, all due to the samples' prior collapse. The double-resistivity jump phenomenon (double-PTC effect) was previously observed by Feng and Chan²² for a similar PP/UHMWPE/CB system and for PVDF/UHMWPE/CB and PVDF/XL-UHMWPE/CB blends.²⁴ Because the first resistivity jump occurred at about 125°C and the second at about 140°C, analogous to the mechanism of the PTC effect in CB-filled single semicrystalline polymers, the first and second PTC effects in the double-PTC effect were attributed to the large thermal expansion resulting from the melting of the UHMWPE (115–135°C) and PP (130–170°C) crystalline phases. A comparison between the 70PP/30XL-UHMWPE blends containing 2 and 4 phr CB showed that the room temperature resistivity of the 4 phr CB blend was lower than the corresponding 2 phr CB blend, as expected. Increasing of the CB content resulted in a sharper (occurring at a narrower temperature region) first PTC, which had decreased intensity and a second PTC intensity increase. The changes in the first PTC characteristics may be explained by the addition of an increasing CB amount into the blend. This may have resulted in a closer interlocking structure between the PE particles and the PP matrix (as was observed for the UHMWPE-containing blends), thus resulting in a smaller and sharper first PTC effect, presumably through

partial inhibition of the XL-UHMWPE particles' expansion. The second PTC intensity increase may be explained by the increased quality and/or quantity of conductive paths that formed within the PP matrix.

This double-PTC effect was previously observed for the PVDF/UHMWPE and PVDF/XL-UHMWPE systems.²⁴ The first PTC, occurring at about the same temperature, was also attributed to the thermal expansion due to melting of the UHMWPE crystalline phase. However, the first PTC intensity was lower for the PP-containing blends than for the PVDF-containing blends whereas the second PTC effect was larger by 3–5 orders of magnitude for the PP-containing systems than for their PVDF-containing counterparts. This difference may be attributed to the different mode of CB distribution and to the different medium through which the conductive networks were established. Thus, the thermal expansion of the CB-containing PP phase due to the melting of PP crystallites was more significant as opposed to PVDF's expansion, influencing CB distribution mainly by exerting pressure on the PE particles. Similar to the previously investigated systems,²⁴ the first PTC effect was not followed by a NTC effect, as usually occurs in CB-filled semicrystalline polymer compounds. Due to the difference in the UHMWPE and PP peak melting temperatures (133 and 158°C, respectively), after the first PTC took place the PP was still mostly in its solid state, and recalling UHMWPE's high viscosity, both effects resulted in the inhibited mobility of the CB particles, partially preventing the formation of new conductive paths. Nevertheless, even if some new conductive paths were formed, their effect should have been nearly negligible, because even after the PE thermal expansion took place, the blends were still highly conductive because of the dominating CB distribution in the PP matrix.

Resistivity–Shear Rate Relationships and Rheological Behavior

The resistivity–shear rate relationship was studied for 70PP/30UHMWPE filaments containing 4 and 6 phr CB that were extruded at 200 (blend compounding temperature), 225, 250, and 275°C. Filaments of 4 phr CB extruded below 275°C maintained high resistivity levels at all shear rates (not shown). The filaments extruded at 275°C had a relatively low resistivity for the low shear rate samples (obtained between ~3 and

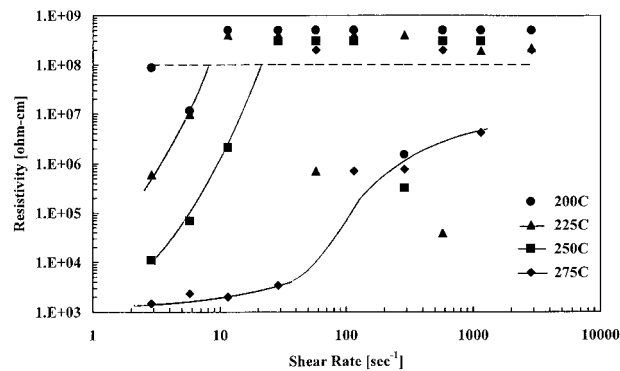


Figure 8 The resistivity versus the extrusion shear rate of 70PP/30UHMWPE/6 phr CB filaments extruded at various temperatures. The data points of resistivity above 1E8 ohm-cm exceeded the range of the measuring equipment and are depicted for illustration purposes only.

~12/s), increasing steeply at the higher shear rates and showing a resistivity drop for the maximum attainable shear rate. This trend was further manifested by the filaments containing 6 phr CB, which are shown in Figure 8. The resistivity at low shear rates decreased with increasing extrusion temperatures, remaining more stable at the higher shear rate levels. Above the intermediate shear rates, the resistivities of all filaments depicted unpredictable trends; at high shear rates, all samples were highly resistive. This experiment was held twice, showing unpredictable trends in both trials.

As depicted in Figure 9, the resistivity–shear rate relationships of 2 and 4 phr CB content 70PP/30XL-UHMWPE blends extruded at the same temperatures (200, 225, 250, and 275°C) were different than their as-received UHMWPE counterpart blends. Both the 2 and 4 phr CB blends were highly resistive when extruded at 200°C. However, as the extrusion temperature of the 4 phr CB blend was increased, the resistivity at low shear rates decreased abruptly. As the shear rate increased, the resistivity of all samples exhibited a moderate resistivity increase up to a shear rate where the samples became highly resistive. The shear rate level at which the samples were no longer conductive increased with increasing extrusion temperature; thus, the sample extruded at 275°C was conductive up to the maximum shear rate. Hence, as the filament extrusion temperature was increased the stability at higher shear rates was enhanced. The 6 phr CB blends extruded at the same temperatures (200, 225,

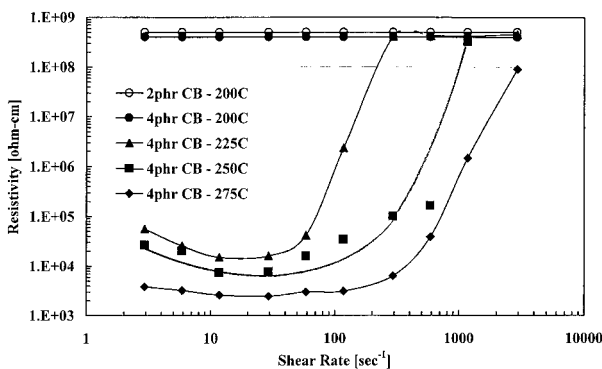


Figure 9 The resistivity versus the extrusion shear rate of 2 and 4 phr CB containing 70PP/30XL-UHMWPE filaments extruded at 200°C and at various temperatures, respectively. The data points of resistivity above 1E8 ohm-cm exceeded the range of the measuring equipment and are depicted for illustration purposes only.

250, and 275°C) were almost indifferent to the shear rate at all temperatures, as shown in Figure 10. However, even at this relatively high CB content, the sample that had the lowest resistivity at all shear rates and that was the least affected by shear rate was the sample extruded at 275°C.

These data may be closely related to the blend morphology. The morphology depicted by the dispersed XL-UHMWPE particles in the blend provided a developed interface in which the CB could locate. The fixation of the UHMWPE particle morphology results in a porous structure into which the PP penetrates, thus inducing an interlocking structure (as previously shown), which may also induce entrapment of the CB particles in the heterogeneous interface areas.²⁶ Thus, the CB regions of low mobility withstood excessive shearing, resulting in only a mild deformation of the developed XL-UHMWPE particle exterior, ascribed also to the particles' "infinite" viscosity, as shown in Figure 11(c,d) in comparison to Figure 11(a,b), although the shear rates were increased. Therefore, it was reasonable to assume that the resistivity decrease at the higher shear rates was mostly due to the deagglomeration of CB clusters, resulting in a finer, more uniform CB dispersion in the PP phase. The PP/UHMWPE/CB blend presented a different morphology than its XL-UHMWPE counterpart, as presented by the model in Figure 5. Thus, the CB was located in the PE particle exterior region and in the PP matrix. However, as was previously stated by Breuer et al.²⁶ regarding a high-impact polystyrene/

UHMWPE system, the UHMWPE particle surface is a uniform region in which the CB particles are distributed more homogeneously. Hence, the CB network is more susceptible to disconnections due to shearing, and only at high CB contents may it obtain low resistivity values at higher shear rates.

The effect of the increasing temperature on the resistivity was analyzed in light of the rheological behavior of the blends. As a result of the increasing temperature, shear stress levels were decreased due to reduced blend viscosity (Figs. 12, 13). Because high viscosity induces disconnection of conductive networks, the lower viscosity exhibited by the blend resulted in electrical stability through wider shear rate levels.

The apparent viscosity of the 4 and 6 phr CB content 70PP/30UHMWPE and 70PP/30XL-UHMWPE blends extruded at 200, 225, 250, and 275°C is depicted in Figures 12 and 13, respectively. All blends exhibited a typical pseudoplastic behavior, in which the XL-UHMWPE blends had a lower apparent viscosity than their as-received UHMWPE counterparts extruded at the same temperature. The difference in apparent viscosity was larger at low shear rates and gradually decreased with increasing shear rate levels. This trend was more obvious for the 4 phr CB blends (Fig. 12) than for the 6 phr CB blends (Fig. 13), which generally exhibited a narrower viscosity range (at a particular shear rate) than their 4 phr CB filled counterparts. Generally, the addition of crosslinked particles results in increased viscosity with increasing crosslinking density.²⁷ However, the as-received UHMWPE and the XL-UHMWPE containing blends showed different trends, attributed to different types of flow mechanisms. The XL-UHMWPE particles lost their

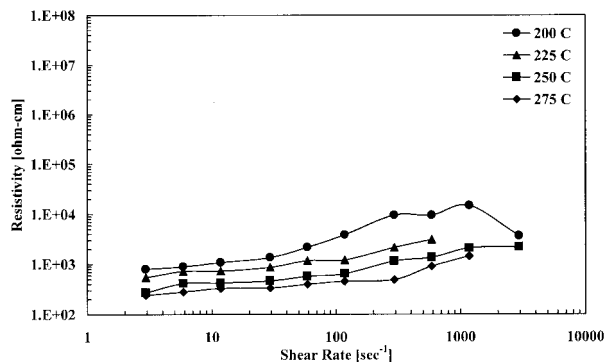


Figure 10 The resistivity versus the extrusion shear rate of 70PP/30XL-UHMWPE/6 phr CB filaments extruded at various temperatures.

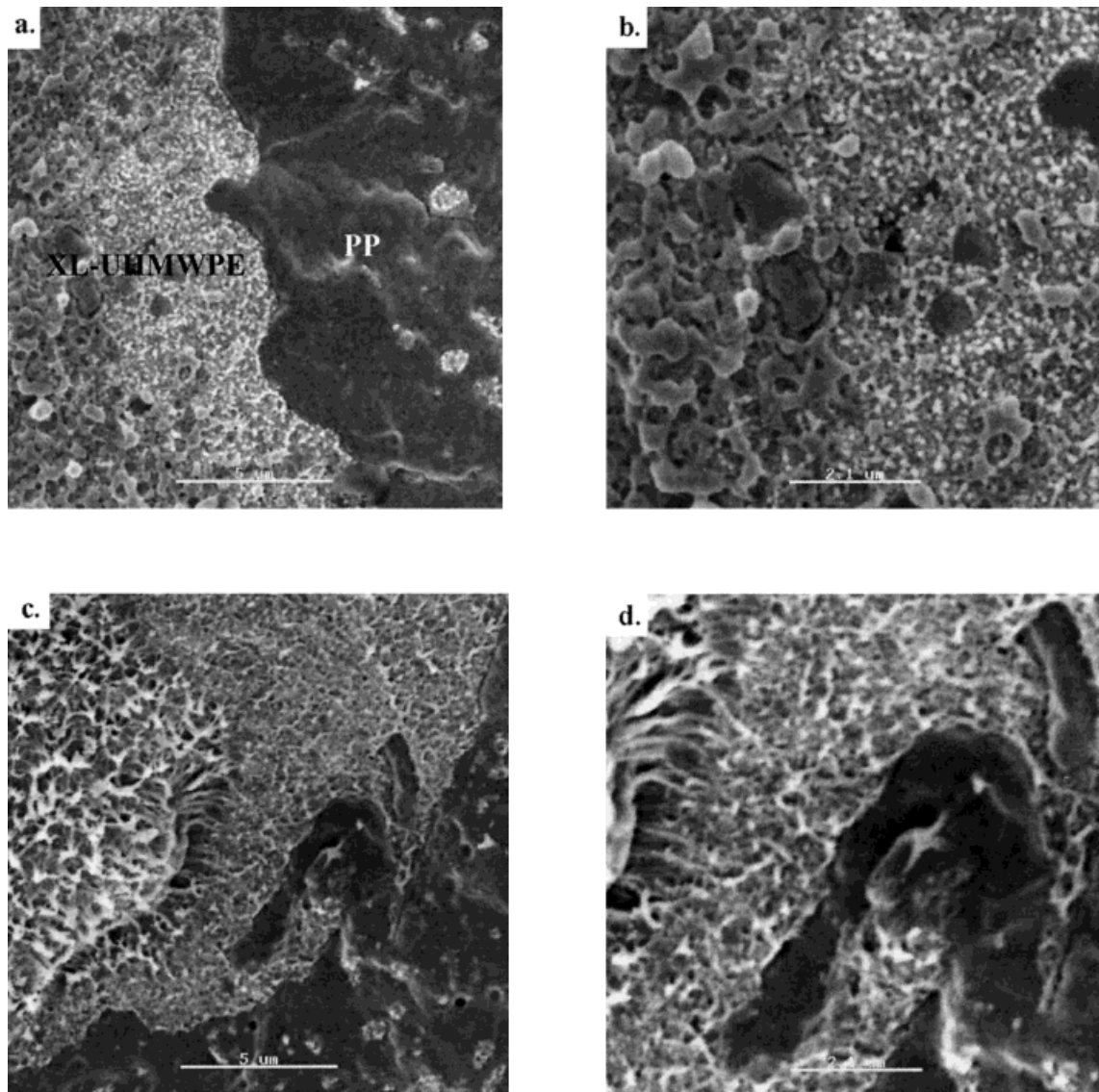


Figure 11 SEM micrographs of a freeze fractured 70PP/30XL-UHMWPE/4 phr CB blend extruded at 275°C: (a,b) at low shear rates, transverse to the flow direction, at two magnifications, and (c,d) at high shear rates, parallel to the flow direction, at two magnifications.

polymer flow properties due to crosslinking⁷ and served as supermolecular flow units, which may also rotate as elastic solid bodies, maintaining their identity and shape.²⁸ Thus, slippage, which is favored by large size and fillerlike particles, prevailed, and the melt viscosity did not play any role in the flow mechanism. On the other hand, the extremely high viscosity UHMWPE particles deformed, as is typical of polymers in a shear field.⁷ Furthermore, interdiffusion and entangling of chain segments across particle boundaries may oppose slippage and increase melt vis-

cosity.²⁹ Such entangling and interdiffusion of chain segments were observed along the boundaries of the UHMWPE particle and PP matrix, making it hard to distinguish between the two phases, as previously discussed and depicted in Figure 3.

The difference between the 4 and 6 phr CB containing blends was suggested to be the result of the CB distribution in the blend. It is known that the inclusion of filler particles in general and CB in particular increases the blend apparent viscosity.^{27,30} As previously observed, as the CB

content increased above a certain level, it predominantly distributed in the PP matrix. Thus, the influence of the CB-filled matrix increased, increasing the apparent viscosity and decreasing the dominance of the XL-UHMWPE particle slippage effect for the 6 phr CB filled blend.

In a future article poly(4-methyl pentene-1) (TPX)/UHMWPE/CB and TPX/XL-UHMWPE/CB ternary systems will be discussed in regard to their electrical, morphological, and thermoelectric behavior and the interrelations thereof.

CONCLUSIONS

The CB particles are attracted to UHMWPE particles, slightly penetrating their external layer and forming a core-shell morphology. The fixated and somewhat porous structure of the XL-UHMWPE particles results in a developed surface into which the PP matrix and CB particles can very slightly penetrate. After covering all PE surfaces, CB particles distribute in the PP matrix. Thus, conductivity is established through CB paths in the PP matrix, interconnecting the CB-covered UHMWPE particles. This particular CB distribution results in the following effects:

1. All studied blends exhibit a double-PTC phenomenon. The first PTC is attributed to the thermal expansion due to melting of the UHMWPE particles while the second

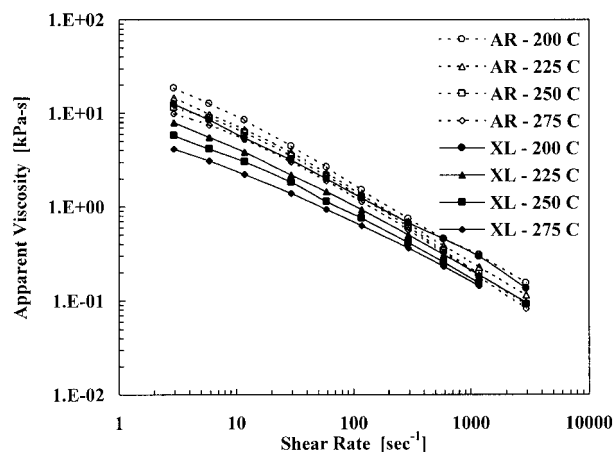


Figure 12 The apparent viscosity versus the shear rate of 70PP/30UHMWPE/4 phr CB (AR) and 70PP/30XL-UHMWPE/4 phr CB (XL) blends extruded at various temperatures.

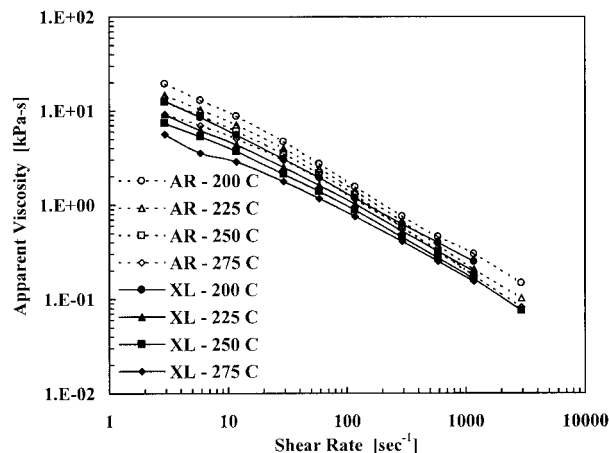


Figure 13 The apparent viscosity versus the shear rate of 70PP/30UHMWPE/6 phr CB (AR) and 70PP/30XL-UHMWPE/6 phr CB (XL) blends extruded at various temperatures.

PTC is related to the melting of the PP matrix.

2. The PP/UHMWPE/CB capillary rheometer filaments exhibit unpredictable resistivities beyond certain levels of shear rates, while their PP/XL-UHMWPE/CB counterpart blends depict more stable trends. Higher filament production temperatures lead to better electrical stability. The different electrical properties of filaments are also related to differences in the rheological behavior of PP/UHMWPE and PP/XL-UHMWPE blends.

REFERENCES

1. Medalia, A. I. *Rubber Chem Technol* 1986, 59, 432.
2. Gubbels, F.; Jerome, R.; Teyssie, P.; Vanlathem, E.; Deltour, R.; Calderone, A.; Parente, V.; Bredas, J. L. *Macromolecules* 1994, 27, 1972.
3. Sumita, M.; Sakata, K.; Asai, S.; Miyasaka, K.; Nakagawa, H. *Polym Bull* 1991, 25, 265.
4. Sumita, M.; Asai, S.; Miyadera, N.; Jojima, E.; Miyasaka, K. *Colloid Polym Sci* 1986, 264, 212.
5. Tchoudakov, R.; Breuer, O.; Narkis, M.; Siegman, A. *Polym Networks Blends* 1996, 6, 1.
6. Lee, B.-L. *Polym Eng Sci* 1992, 32, 36.
7. Breuer, O.; Tzur, A.; Narkis, M.; Siegman, A. *J Appl Polym Sci* 1999, 74, 1731.
8. Narkis, M.; Ram, A.; Flashner, F. *Polym Eng Sci* 1978, 18, 649.
9. Narkis, M.; Ram, A.; Stein, Z. *J Appl Polym Sci* 1980, 25, 1515.

10. Narkis, M.; Vaxman, A. *J Appl Polym Sci* 1984, 29, 1639.
11. Al-Allak, H. M.; Brinkman, A. W.; Woods, J. *J Mater Sci* 1993, 28, 117.
12. Chen, X. B.; Issi, J.-P.; Cassart, M.; Devaux, J.; Billaud, D. *Polymer* 1994, 35, 5256.
13. Meyer, J. *Polym Eng Sci* 1974, 14, 706.
14. Meyer, J. *Polym Eng Sci* 1973, 13, 462.
15. Ohe, K.; Naito, Y. *Jpn J Appl Phys* 1971, 10, 99.
16. Klason, C.; Kubat, J. *J Appl Polym Sci* 1975, 19, 831.
17. Voet, A. *Rubber Chem Technol* 1981, 54, 42.
18. Feng, J.; Chan, C.-M. *Polym Eng Sci* 1999, 39, 1207.
19. Wu, C.; Asai, S.; Sumita, M. *Sen-I Gakkaishi* 1993, 49, 103.
20. Feng, J.; Chan, C.-M. *Polym Eng Sci* 1998, 38, 1649.
21. Tang, H.; Liu, Z. Y.; Piao, J. H.; Chen, X. F.; Lou, Y. X.; Li, S. H. *J Appl Polym Sci* 1994, 51, 1159.
22. Feng, J.; Chan, C.-M. ANTEC '99; New York, 1999; p 2766.
23. Halldin, G. W.; Kamel, I. L. *Polym Eng Sci* 1977, 17, 21.
24. Mironi-Harpaz, I.; Narkis, M. *Polym Eng Sci* 2001, 41, 205.
25. Wu, S. *Polymer Interface and Adhesion*; Marcel Dekker: New York, 1982.
26. Breuer, O.; Tcoudakov, R.; Narkis, M.; Siegmann, A. *Polym Eng Sci* 2000, 40, 1015.
27. Gandhi, K.; Park, M.; Sun, L.; Zou, D.; Li, C. X.; Lee, Y. D.; Aklonis, J. J.; Salovey, R. *J Polym Sci Part B Polym Phys* 1990, 28, 2707.
28. Swanson, C. L.; Fanta, G. F.; Bagley, E. B. *Polym Compos* 1984, 5, 52.
29. Berens, A. R.; Folt, V. L. *Polym Eng Sci* 1969, 9, 27.
30. Joo, Y. L.; Lee, Y. D.; Kwack, T. H.; Min, T. I. ANTEC '96; 1996; Indianapolis, IN p 64.